IET Generation, Transmission & Distribution

Research Article

IET Journals
The Institution of Engineering and Technology

Adaptive distance protection scheme for shunt-FACTS compensated line connecting wind farm

ISSN 1751-8687
Received on 24th June 2015
Revised on 25th August 2015
Accepted on 6th September 2015
doi: 10.1049/iet-gtd.2015.0775
www.ietdl.org

Rahul Dubey[1], *Subhransu Ranjan Samantaray*[2] ✉, *Bijay Ketan Panigrahi*[1]

[1]*Department of Electrical Engineering, Indian Institute of Technology, Delhi, India*
[2]*Schools of Electrical Sciences, Indian Institute of Technology, Bhubaneswar, India*
✉ *E-mail: sbh_samant@yahoo.co.in*

Abstract: To improve the performance of the conventional distance protection scheme for compensated lines with high resistance faults, an adaptive distance protection scheme is proposed. This study presents an analytical approach for finding the possible impacts of shunt connected flexible AC transmission systems (FACTS) devices such as static synchronous compensator/static volt-ampere reactive (VAR) compensator (SVC) integrated with off-shore wind farm (WF) on distance relay characteristics. Analytical results are presented and verified on simulation platform compares under reach phenomena in presence of both FACTS devices and it is found that under reach is more severe for SVC connected system. Moreover, presence of SVC changes the line characteristic presented to relay even for bolted faults. It is also seen that type of coupling transformer has a considerable effect on apparent impedance. Furthermore, the reach setting of the relay is significantly affected as the relay end voltage and power fluctuates continuously (due to non-linear relationship with speed) when off-shore WFs are connected to power transmission systems. Thus, adaptive tripping characteristics for high resistance line-to-ground fault with shunt-FACTS devices considering appropriate operating conditions is a demanding concern and the same has been addressed in the proposed research work.

Nomenclature

x	fault location
R_f	fault resistance
I_f	fault current
$V_{prefault\_f}$	pre-fault voltage
$V_{postfault\_R}$	post-fault voltage
I_{relay}	relay current
Z_1, Z_2 and Z_0	positive, negative and zero sequence equivalent impendences
Z_{1s}, Z_{2s} and Z_{0s}	positive, negative and zero sequence sending end source impendences
Z_{1r}, Z_{2r} and Z_{0r}	positive, negative and zero sequence receiving end source impendences
I_1, I_2 and I_0	positive, negative and zero sequence currents
V_{ref} and V_{HV}	reference and high voltage for SVC
Z_{xr0}	zero sequence shunt impedance of SVC
Z_{SVC}	equivalent impedance of SVC
$Z_{STATCOM}$	equivalent impedance of STATCOM
$Z_{APPARENT}$	equivalent apparent impedance

1 Introduction

In recent years, there has been an intensive effort to increase the participation of renewable sources of electricity in the fuel and energy balance of many countries. In particular, this relates to the power of wind farms (WFs) attached to the power system at both the distribution network and the high-voltage (HV) transmission network. The number and the level of power of off-shore WF integration in the power system are growing steadily which increases participation and the role of such sources in the overall energy balance. Incorporating wind energy sources into the power system entails a number of new challenges for the power system protections in that it will have an impact on distance protections which use the impedance criteria as the basis for decision making. The most difficult part in WF is the uncontrolled wind speed, leading to voltage, power and frequency fluctuations. Thus, the protection issues become critical as the transmission lines connecting WFs are subjected to continuously changing environment. Adaptive protection schemes for distribution [1–3] and transmission lines [4–6] including WF are proposed and the effect of variations in wind-farm parameters on the reach setting is extensively studied. It is observed that the trip boundaries of the relay are significantly affected when the loading level, source impedance, voltage level, frequency etc. vary.

Similarly, installation of FACTS devices is one of the solutions for transmission expansion planning (TEP) to meet expected increase in power demand. However, constructions of new transmission line infrastructure of higher capacities are facing stiff resistance from economy involved and environment concerns. Thus, system is being made to operate closer to their stability limit. Installation of FACTS devices cause efficient utilisation of transmission system network by controlling and regulating active and reactive power flows, and can also contribute in enhancing system stability (increasing transient stability and power system oscillation damping [7–15]). In the TEP solutions, the FACTS devices are being installed on existing transmission network, which is by the same distance relay [9]. Adaptive distance relay setting for series compensated line has been discussed in [16]. Recently, the simultaneous impact of unified power flow controller and off-shore wind penetration on distance relay characteristics have been proposed in [17, 18]. Moreover, the adaptive direct under reaching transfer trip protection scheme for three-terminal line discussed in [19]. In [20], a new adaptive distance protection scheme based on voltage drop equation is presented. However, none of the aforementioned research paper discusses adaptive distance relay setting for shunt-FACTS compensated line integrated with WF.

Thus, there is a strong motivation to develop the comprehensive adaptive distance relaying scheme including both shunt-FACTS and WF. The main objective of the proposed research work is to show the effectiveness of the proposed algorithm, using some realistic FACTS device such as static VAR compensator (SVC)/ static synchronous compensator (STATCOM). Therefore, one needs to know the level of under reach caused by such scenarios. The location of shunt connected installation depends on system

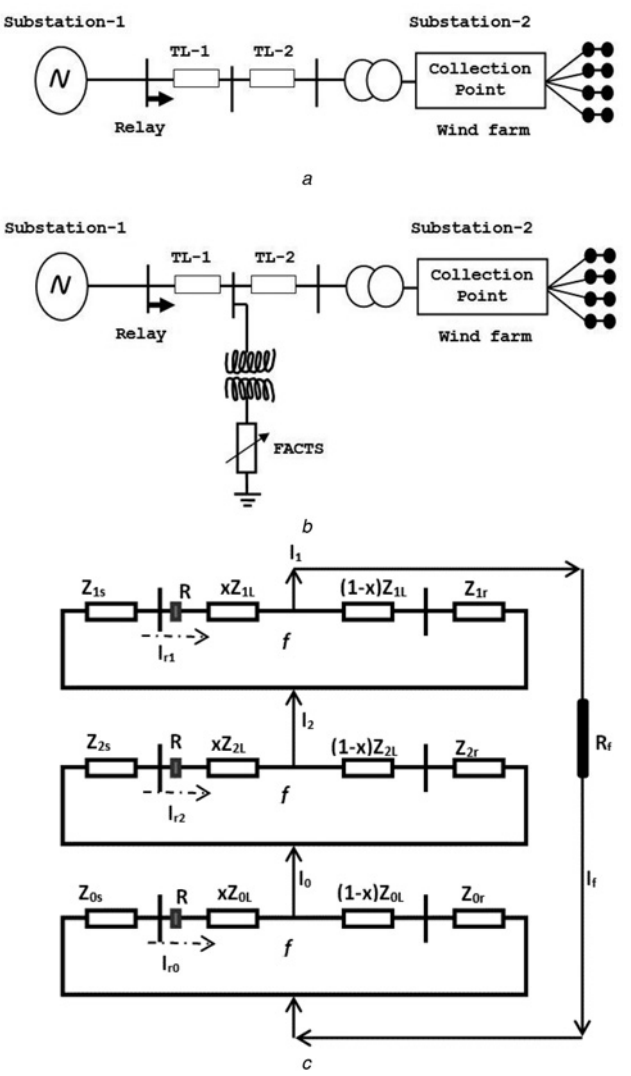

Fig. 1 *System studied*

a Single-line diagram of the studied system with WF
b Single-line diagram of the studied system shunt-FACTS device and WFs
c Sequence network for uncompensated line for A–G fault situation

engineers' requirement. Theoretically, devices can be installed at three locations, that is, at sending end [just after generating station switchyard (i.e. after relay)] or at middle of the transmission line compensation or at receiving end substation. Shunt connected FACTS devices (SVC/STATCOM) are installed at receiving end to increase system stability (improving high-voltage, direct current performance), whereas mid-point compensation is used for increasing power transfer capacity [7–12]. Presently, utilities pay serious attention on the effect of shunt connected FACTS device on distance relay characteristics. Therefore, first two cases, that is, shunt connected FACTS device at sending end and at middle of the line is considered here. The objective of this paper is to (i) observe the distance relay characteristics in presence of shunt-FACTS devices such as SVC/STATCOM, (ii) investigate the impact of SVC and STATCOM on trip region for single-line-to-ground (A–G) faults and (iii) comparison of the results of the analytical and simulation studies draw conclusion. Furthermore, the impact of coupling transformer along with the impact of WFs together with shunt-FACTS devices on reach setting of distance relay is studied.

2 SVC and STATCOM

The characteristics of SVC and STATCOM are very well explained in [7–12]. STATCOM is based on converter technology, whereas

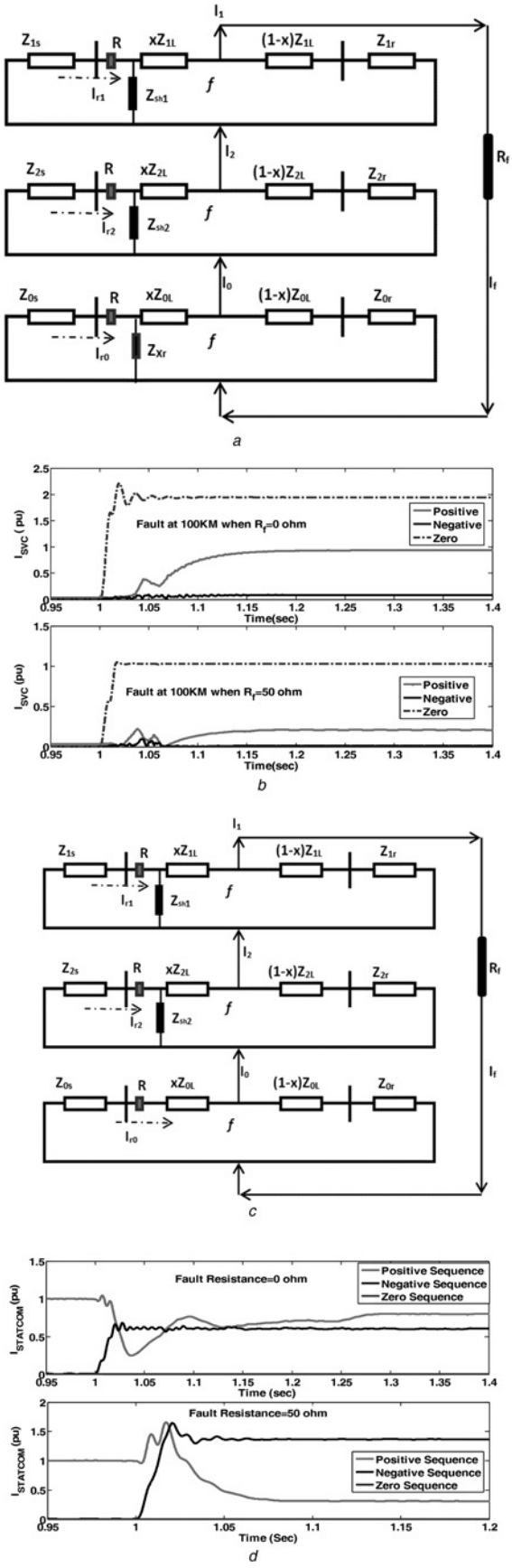

Fig. 2 *Apparent impedance calculation for SVC at sending end*

a Sequence network for shunt compensated (SVC at sending end) line for A–G fault situation
b Sequence current analysis of SVC
c Sequence network for shunt compensated (STATCOM at sending end) line for A–G fault situation
d Sequence current analysis of STATCOM

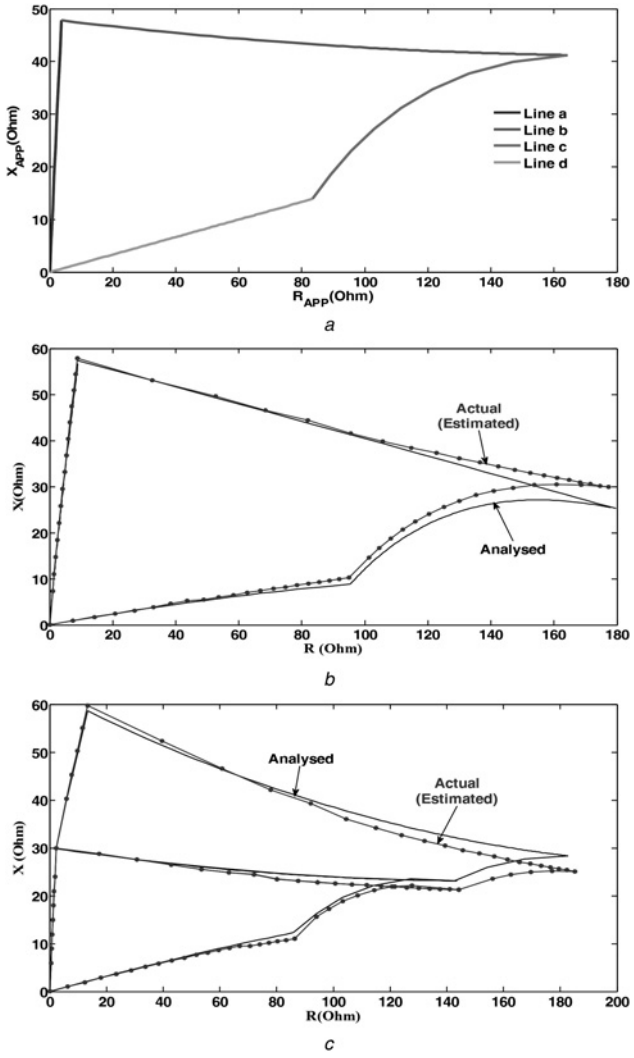

Fig. 3 *Trip region for uncompensated line connected with off-shore WF*

a Impact of off-shore WF on apparent impedance trajectory
b Trip region for SVC (installed at starting of transmission line) shunt compensated line connected with off-shore WF
c Trip region for SVC (installed at starting of transmission line) shunt compensated line connected with off-shore WF

SVC generates/absorbs reactive power through suitable operation of thyristor controlled reactor (TCR) and thyristor switched capacitor (TSC). Therefore, attaining capacitive compensation limit SVC behaves like a capacitor in parallel to system. Furthermore, reduction in voltage at point of connect will reduce reactive power support to grid, whereas STATCOM can supply the rated current support up to 0.15 pu of system voltage [9]. Thus, on reaching capacitive limit, the STATCOM capacitive reactance will continuously reduce to keep capacitive current constant, whereas SVC current reduces as capacitive reactance is fixed. There can be two modes of operation of these FACTS devices, that is, voltage regulation mode and VAR regulation mode. In this paper, the investigations are made with voltage regulation mode.

During fault, the system voltage reduces and thus shunt connected FACTS devices will always supply reactive power during fault. Hence, for network analysis they can be replaced by their minimum capacitive reactance calculated on base value. FACTS devices are installed on transmission lines where load on all three lines are equal for practical consideration. For voltage regulation mode balanced three-phase firing shall be used. In case of unsymmetrical fault, the converter will try regulating all three phases, that is, in order to control any one or two phase, the controller will equally compensate all three phases, and thus there will be increase in healthy phase voltage due to controller action [9]. The amount of capacitive compensation during fault will mainly depend on power flow through lines. Other factors such as system strength, fault resistance also affects compensation.

3 System studied

Fig. 1*a* shows the single-line diagram of the interconnection of WF to the grid without FACTS devices [4, 5]. Fig. 1*b* shows the schematic configuration of the system under study. In this paper, MATLAB/SIMULINK (Sim Power System) is used to model the 500 kV, 300 km long transmission system with STATCOM/SVC and off-shore wind-farm integration. The parameters of the system are as follows.

WF: The 60 MW WF (consists of 40 numbers of 1.5 MW wind turbines) is connected to the substation 1 through 500 kV transmission line. Wind turbines use a double fed induction generator (DFIG) consisting of a wound rotor induction generator and an ac/dc/ac insulated-gate bipolar transistor-based pulse width modulation converter. The details of the wind-farm modelling considered in our proposed relaying scheme are derived from [21–24].

Table 1 Actual against estimated $R_{APP} - X_{APP}$ when SVC installed in sending end

Serial number	Line-a		Line-b		Line-c		Line-d	
	Actual (R_{APP})	Estimated (R_{APP})	Actual (X_{APP})	Estimated (X_{APP})	Actual (R_{APP})	Estimated (R_{APP})	Actual (X_{APP})	Estimated (X_{APP})
1	–	–	57.73991	57.84385	98.45	95.055	–	–
2	0.9177	0.9211	52.88882	53.11625	102.8	101.28	0.914	0.9189
3	1.4052	1.4107	49.27166	49.58208	104.8	104.68	1.688	1.7137
4	1.9105	1.9178	46.23172	46.59696	107.3	108.27	2.409	2.4518
5	2.4322	2.4412	44.00918	44.41847	110.3	112.06	3.080	3.1349
6	2.9773	2.9874	41.12483	41.56076	113.8	116.12	3.810	3.8763
7	3.5311	3.5420	39.41812	39.87143	117.8	120.44	4.519	4.5928
8	4.1125	4.1244	37.99717	38.46074	122.2	125.05	5.197	5.2761
9	4.7066	4.7188	36.81998	37.2876	127.0	130.00	5.402	5.4775
10	5.3077	5.3188	35.72155	36.18594	132.2	135.27	5.931	6.0059
11	5.8947	5.9053	34.81166	35.2677	137.9	140.93	6.442	6.5145
12	6.4743	6.4847	33.95144	34.39621	144.1	147.09	6.910	6.9782
13	7.0586	7.0678	33.26522	33.69435	150.7	153.70	7.349	7.4124
14	7.6271	7.6355	32.57698	32.99397	158.0	160.92	7.775	7.8341
15	8.1816	8.1898	32.03489	32.43853	165.9	168.74	8.202	8.2556
16	8.7068	8.7138	31.50433	31.89499	174.5	177.34	8.586	8.6343
17	–	–	31.07714	31.45629	–	–	8.953	8.9975
18	–	–	30.55243	30.91601	–	–	9.253	9.2939
19	–	–	30.25797	30.60897	–	–	9.606	9.6442
20	–	–	29.81880	30.15278	–	–	9.875	9.9112
21	–	–	29.59389	29.91055	–	–	10.18	10.224

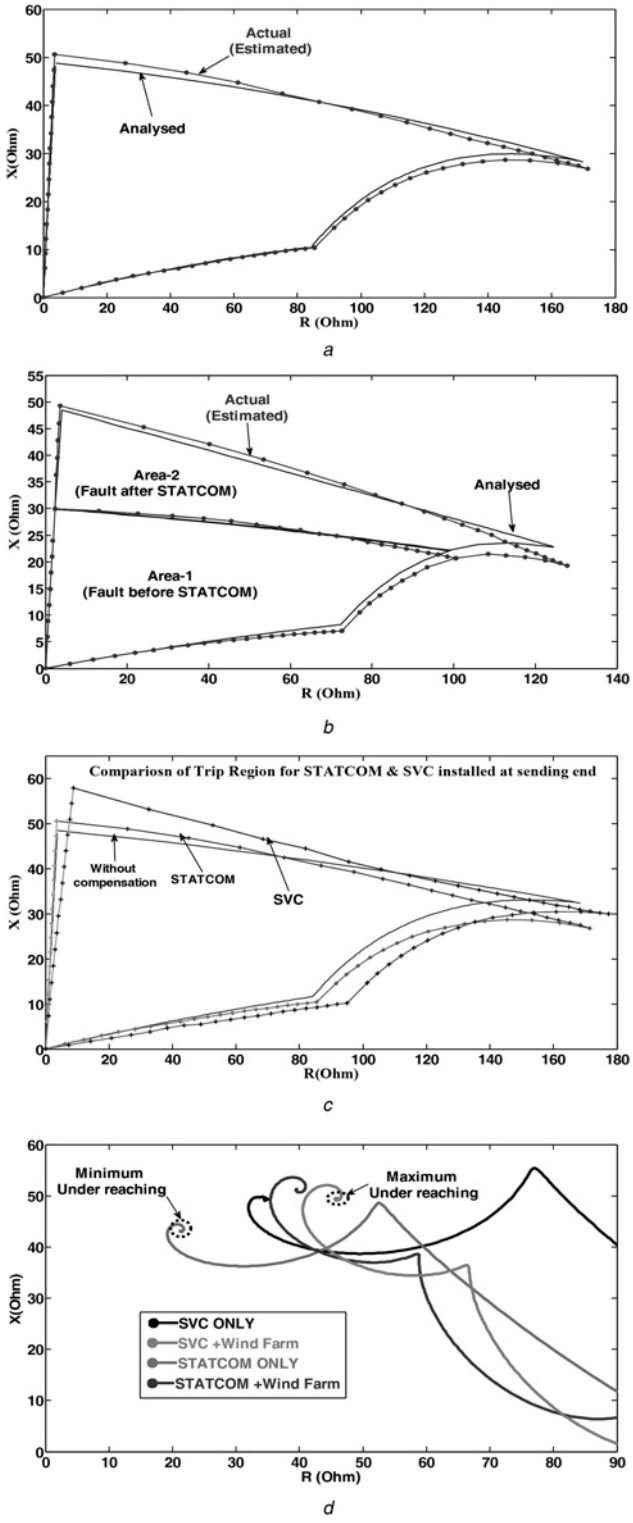

Fig. 4 *Trip region for STATCOM with off-shore WF*

a Trip region for STATCOM (installed at starting of transmission line) shunt compensated line connected with off-shore WF
b Trip region for STATCOM (installed at middle of transmission line) shunt compensated line connected with off-shore WF
c Comparative assessment of SVC against STATCOM installed at relay end
d Trip region for uncompensated line connected with off-shore WF

SVC model: For simulation purpose, the SVC detailed modelled given in SIMULINK/MATLAB R2010a is used. To keep rating as that of STATCOM, the TCR of 100 MVAR and three TSCs of 33.33 MVAR are considered by suitable changes in L and C values. The inductance of TCR is 20.39mH and capacitance of each TSC is 115.17 μf. This is connected to 500 kV system through 500 kV/16 kV (star/delta) 100 MVA, 0.05% impedance whose star side (i.e. 500 kV side) is solidly grounded.

STATCOM model: For simulation purpose, the STATCOM detailed modelled given in SIMULINK/MATLAB R2010a is used. It is based on 48 pulse voltage source inverter. This is connected to system through secondary side series connected four numbers of 25 MVA 0.05 pu% impedance transformer. The secondary of all transformers are in zigzag formation though solidly grounded on one point.

4 Apparent impedance measurement

4.1 Apparent impedance calculation for uncompensated line

For Fig. 1*a*, the sequence network for A–G fault is shown in Fig. 1*c* where $V_{\text{prefault\_f}}$ is pre-fault voltage at f point, $I_{\text{prefault\_R}}$ is load current seen by relay before fault and $V_{\text{postfault\_R}}$ is post-fault voltage seen by relay. 1, 2 and 0 denote positive sequence, negative sequence and zero sequence quantities. The detailed derivation of apparent impedance calculation for uncompensated line is given in Appendix 1.

4.2 Apparent impedance calculation for SVC at sending end

Equations (12)–(31) present the apparent impedance calculation for transmission line with SVC installed at relay end. For Fig. 1*b* with SVC, the sequence network or A–G fault is given in Fig. 2*a*. The detailed derivation of apparent impedance calculation for SVC at sending end is given in Appendix 2. Fig. 2*b* shows the sequence current of SVC during fault. The conclusion drawn from Fig. 2*b* is as follows: (i) the zero sequence current is highly pronounced, whereas the same is absent in case of STATCOM. It can be interpreted that the zero sequence impedance of SVC is different from positive/negative sequence impedance. The explanation of same lies in the type of coupling transformer which is star and solidly grounded on 500 kV side. Thus, capacitive reactance will not be present and zero sequence impedance of SVC will be simply that of coupling transformer only and (ii) for bolted faults, the fault current supplied by SVC is more as compared with supplied by STATCOM.

4.3 Apparent impedance calculation for STATCOM at sending end

Equations (32)–(51) present the apparent impedance calculation for transmission line with STATCOM installed at relay end. For Fig. 1*b* with STATCOM, the sequence network for A–G fault is shown in Fig. 2*c*. The detailed derivation of apparent impedance calculation for STATCOM at sending end is given in Appendix 3. Fig. 2*d* shows the sequence current of SVC during fault. The conclusions drawn from Fig. 2*d* are as follows: (i) zero sequence current through STATCOM during fault is zero. It is because of coupling transformer. Hence zero sequence network of STATCOM is open at point where it is installed and (ii) as the fault resistance increases, the negative sequence current dominates the positive sequence current and this factor may be utilised for protection of STATCOM.

5 Trip region analysis

5.1 Trip region for uncompensated line connected with off-shore WF

The apparent impedance calculation for uncompensated transmission line connected with off-shore WF for A–G fault has been discussed in Section 4. Fig. 3*a* shows the trip region for uncompensated line, where the four lines and the included area for an ideal trip region defined below:

Table 2 Actual against estimated $R_{APP} - X_{APP}$ when STATCOM installed in sending end

Serial number	Line-a		Line-b		Line-c		Line-d	
	Actual (R_{APP})	Estimated (R_{APP})	Actual (X_{APP})	Estimated (X_{APP})	Actual (R_{APP})	Estimated (R_{APP})	Actual (X_{APP})	Estimated (X_{APP})
1	0.4232	0.4243	50.52284	50.61379	88.44	85.397	–	–
2	0.6345	0.6369	48.57906	48.78795	92.92	91.487	1.065	1.0711
3	0.8463	0.8497	46.51966	46.81274	94.94	94.820	2.018	2.0484
4	1.0567	1.0608	44.33756	44.68783	97.56	98.425	2.894	2.9444
5	1.2696	1.2743	42.09594	42.48744	100.6	102.23	3.703	3.7696
6	1.4874	1.4925	40.29006	40.71714	104.2	106.35	4.386	4.4625
7	1.7111	1.7165	38.76857	39.21441	108.3	110.74	4.957	5.0378
8	1.9360	1.9417	37.32172	37.77705	112.8	115.48	5.479	5.5620
9	2.1567	2.1624	35.98334	36.44033	117.7	120.51	5.996	6.0788
10	2.3809	2.3864	34.73615	35.18773	123.1	125.92	6.520	6.6020
11	2.6128	2.6183	33.67726	34.11844	129.1	131.91	7.031	7.1093
12	2.8158	2.8209	32.60564	33.03278	135.5	138.29	7.481	7.5545
13	3.0637	3.0687	31.74015	32.1496	142.7	145.46	7.922	7.9910
14	3.2881	3.2924	31.00308	31.39992	150.5	153.28	8.313	8.3757
15	3.5272	3.5311	30.19324	30.57368	159.1	161.85	8.679	8.7360
16	–	–	29.54362	29.90997	168.7	171.45	9.008	9.0594
17	–	–	28.84838	29.20034	–	–	9.333	9.3793
18	–	–	28.21498	28.55074	–	–	9.647	9.6898
19	–	–	27.62087	27.94128	–	–	9.903	9.9420
20	–	–	27.14026	27.44424	–	–	10.16	10.201
21	–	–	26.54997	26.83406	–	–	10.38	10.423

Line-a: Solid faults at different locations.
Line-b: Faults at a relay-reach end (80% of line length) with different fault resistances up to 200 Ω.
Line-c: Faults at different points with a 200 Ω fault resistance.
Line-d: Faults at the relaying point with different fault resistances up to 200 Ω.

5.2 Trip region for SVC with off-shore WF

The apparent impedance calculation for shunt compensated (with SVC) transmission line connected with off-shore WF for A–G fault has been discussed in Section 4. Fig. 3*b* shows the trip region for with SVC installed at the starting of transmission line. Fig. 3*c* shows the trip region for with SVC installed at middle of transmission line. Thus, from Figs. 3*b* and *c* it is observed that when the SVC is installed at sending end, only one trip zone (area-1) comes into picture (the reason being fault always including SVC). Similarly, when SVC is installed at the middle of the line, two trip zones (area-1 and area-2) are generated: area-1 for the fault not including SVC and area-2 for fault including SVC. Summary of the actual and estimated apparent impedance at given operating conditions of SVC are presented in Table 1.

5.3 Trip region for STATCOM with off-shore WF

The apparent impedance calculation for shunt compensated (with STATCOM) transmission line connected with off-shore WF for A–G fault has been discussed in Section 4. Fig. 4*a* shows the trip region for with STATCOM installed at starting of transmission line. Fig. 4*c* shows the trip region with STATCOM installed at middle of transmission line. Summary of the actual and estimated apparent impedances at given operating conditions of STATCOM are presented in Table 2.

5.4 Trip region for SVC against STATCOM with off-shore wind penetration

The comparative assessment of adaptive distance relay setting in presence of SVC/STATCOM and uncompensated transmission network is presented in Fig. 4*c*. From Fig. 4*c*, it is observed that there is only one tripping boundary area existing when SVC and STATCOM are installed at relay location because fault always includes SVC/STATCOM. Again the coupling transformer affects the trip region for SVC and STATCOM as no zero sequence current flows through SVC/STATCOM during healthy and fault condition. Moreover, the tripping area of SVC is more than the tripping area of STATCOM during A–G fault situation which causes the relay to under reach severely in case of SVC compared with that of STATCOM. Again, in Fig. 4*c*, theoretical against estimated boundary from simulation model is presented which clearly indicates the effectiveness of the proposed adaptive distance relay setting method.

6 Performance measurement and comparative assessment of the proposed distance relay characteristics

6.1 Impact of off-shore WF on the distance relay performance and validation on real-time platform

Wind speed varies continuously throughout a day resulting in fluctuating wind-farm output power. When such a farm is connected to the grid through a line with SVC/STATCOM, the transmitted power and the relay end voltage (with respect to grid voltage) fluctuate continuously. The output power of a generating unit has a non-linear relationship with the wind speed (i.e. $P_m \alpha V_w^3$, where P_m is the power extracted from the wind in watts; V_w (m/s) is wind speed at hub height upstream of the rotor). Therefore, the frequency and voltage fluctuation happens due to speed variation [17, 18]. The impact of off-shore WF on apparent impedance trajectory for A–G fault after SVC and STATCOM is shown in Fig. 4*d*. From Fig. 4*d*, it is observed that the apparent impedance value is maximum in case of off-shore WF with SVC compared with SVC only. Similarly, apparent impedance value maximum in the case of off-shore WF with STATCOM compared with STATCOM only. Therefore, the addition of off-shore WF to shunt-FACTS (i.e. SVC/STATCOM) compensated transmission line increases the under reaching effect.

The experimental validation is carried out on OPAL-RT eMEGAsim real-time simulator OP5600 platform. The simulator contains a powerful real-time target computer equipped with up to 12, 3.3 GHz processor cores with a real-time operating system from QNX and Red Hat Linux. RT-LAB software is a distributed real-time platform fully integrated with MATLAB/SIMULINK. It is the software that is used to conduct real-time simulation of SIMULINK models in an OPAL-RT module. Figs. 5*a–c* show the impedance trajectory during ground fault (A–G type) for different fault resistances on OPAL-RT platform. Fig.5*d* presents the OPAL-RT setup.

6.2 Proposed adaptive distance protection scheme in presence of shunt-FACTS devices

To achieve an accurate adaptive relay setting for the distance relay in presence of the WF, information from both ends are required. The

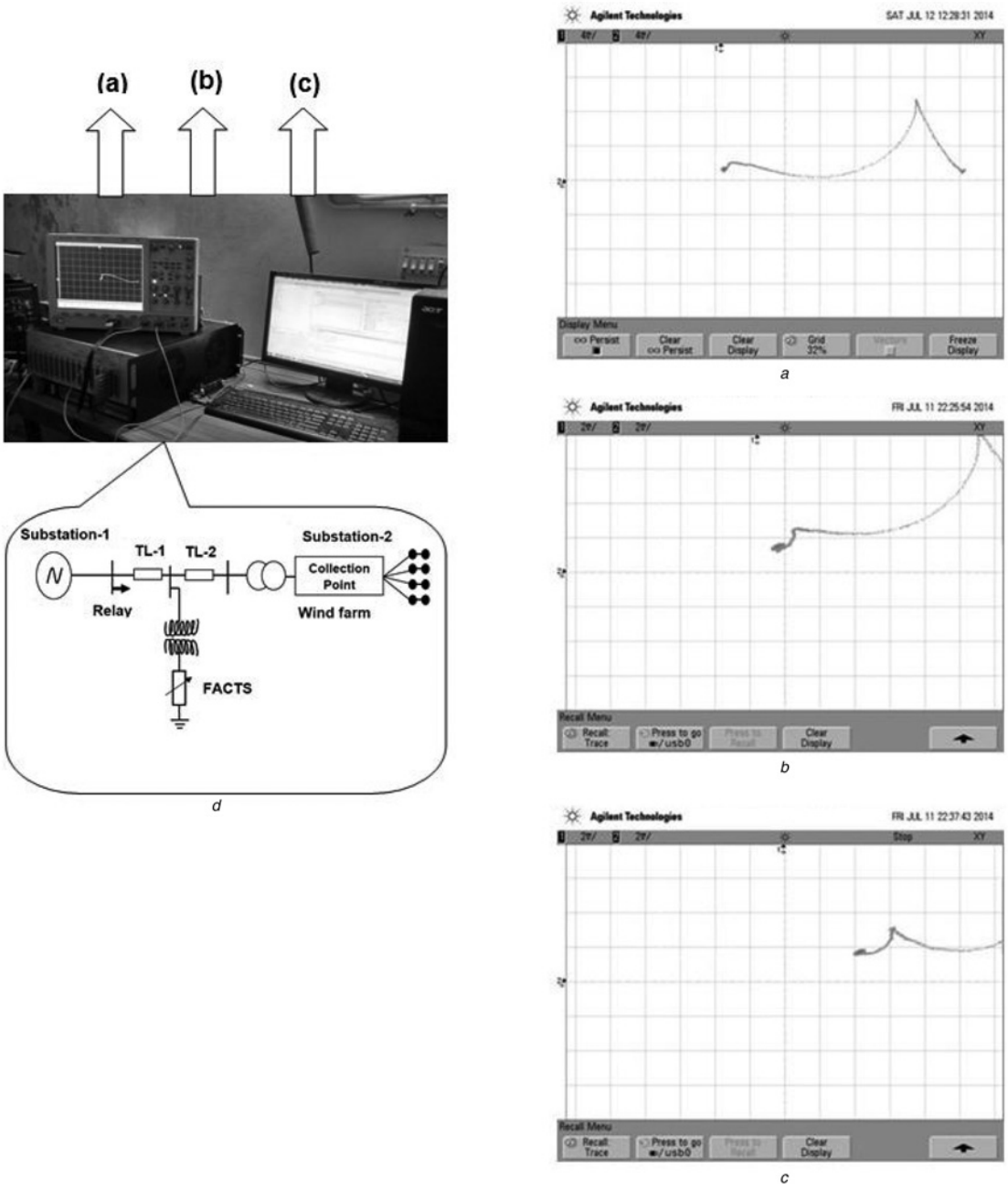

Fig. 5 *Impedance trajectory during AG fault in real-time platform*

a 1 Ω
b 20 Ω
c 75 Ω
d OPAL-RT setup

wind-farm side voltage, current information are necessary to compute the apparent impedance. The flowchart of the proposed adaptive relay setting algorithm is shown in Fig. 6 for developing the relay tripping characteristics.

6.3 Effect of fault resistance in presence of SVC installed in relay end

When an A–G fault with fault resistances 10 and 70 Ω is on the right side of SVC (i.e. at a fault distance of 150 km from the relay point) and the desired voltage, the apparent impedance trajectory seen by the A–G element of the system with and without WF for the distance relay with conventional mho or conventional quadrilateral characteristic are as shown in Fig. 7*a*.

The corresponding apparent impedance trajectory for A–G fault of fault resistances 10 and 70 Ω with and without WF also observed in Fig. 7*b*. From the above, it can be seen that in both the cases, that is, SVC alone and SVC with WF, power system during A–G fault of fault resistances 10 and 70 Ω, the conventional mho or conventional quadrilateral relay is unable to trip or cause the distance relay to under reach. However, the proposed distance relay characteristics shown in Fig. 7*b* works effectively. Table 3 presents the performance measurements of the proposed scheme in presence of SVC with effect of fault resistance.

6.4 Effect of fault location in presence of SVC installed in middle of the line

To study the coverage of the conventional mho, conventional quadrilateral and the proposed distance relay characteristic, faults at different positions have been studied. The distance relay conventional mho or conventional quadrilateral characteristic for

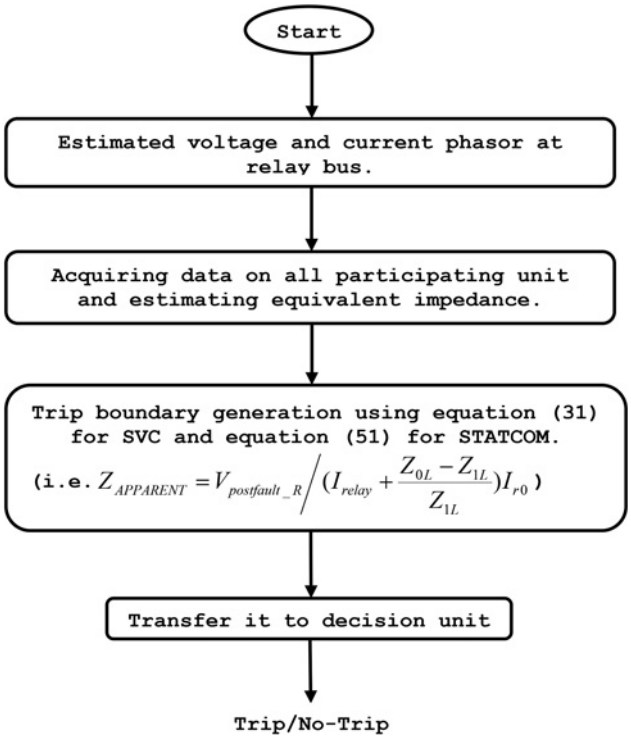

Fig. 6 *Flowchart for trip boundary generation by the proposed method*

A–G fault with and without WF is shown in Fig. 7*c*. It is apparent that when the fault is on the left side of SVC (i.e. before SVC), the apparent impedance seen by the distance relay is almost the same as that for the system without SVC. However, when the fault is on the right side of SVC (i.e. after SVC), both the apparent resistance and reactance of the system with SVC are larger than for the system without SVC. This happens as due to the reactive power injection by SVC, the voltage at the SVC connecting point is higher compared with the system without SVC, that is, as seen by the distance relay, the fault is further away than the real distance. An increase in the apparent impedance will lead to the under reaching of distance relay. The proposed distance relay characteristics shown in Fig. 7*d* and works effectively during the aforementioned conditions. Table 4 presents the performance measurements of the proposed scheme in presence of SVC with effect of fault location.

6.5 Effect of fault resistance in presence of STATCOM installed in relay end

When an A–G fault with resistances 15 and 85 Ω is on the right side of STATCOM, that is, at a fault distance of 150 km from the relay point, and the desired voltage, the apparent impedance trajectory seen (with and without WF together) by the conventional mho or quadrilateral characteristic are as shown in Fig. 8*a*. The corresponding apparent impedance trajectory for A–G fault with fault resistances 10 and 70 Ω with and without WF is shown in Fig. 8*a*. From the above, it can be seen that in both the cases, that is, STATCOM alone and STATCOM with WF during A–G fault with fault resistances 15 and 85 Ω, the conventional mho or conventional quadrilateral are unable to trip or under reach. However, the proposed distance relay characteristics shown in Fig. 8*b* works effectively. Table 5 presents the performance measurements of the proposed scheme in presence of STATCOM with effect of fault resistance.

6.6 Effect of fault location in presence of STATCOM

To study the coverage of the conventional mho, conventional quadrilateral and the proposed distance relay characteristic, faults

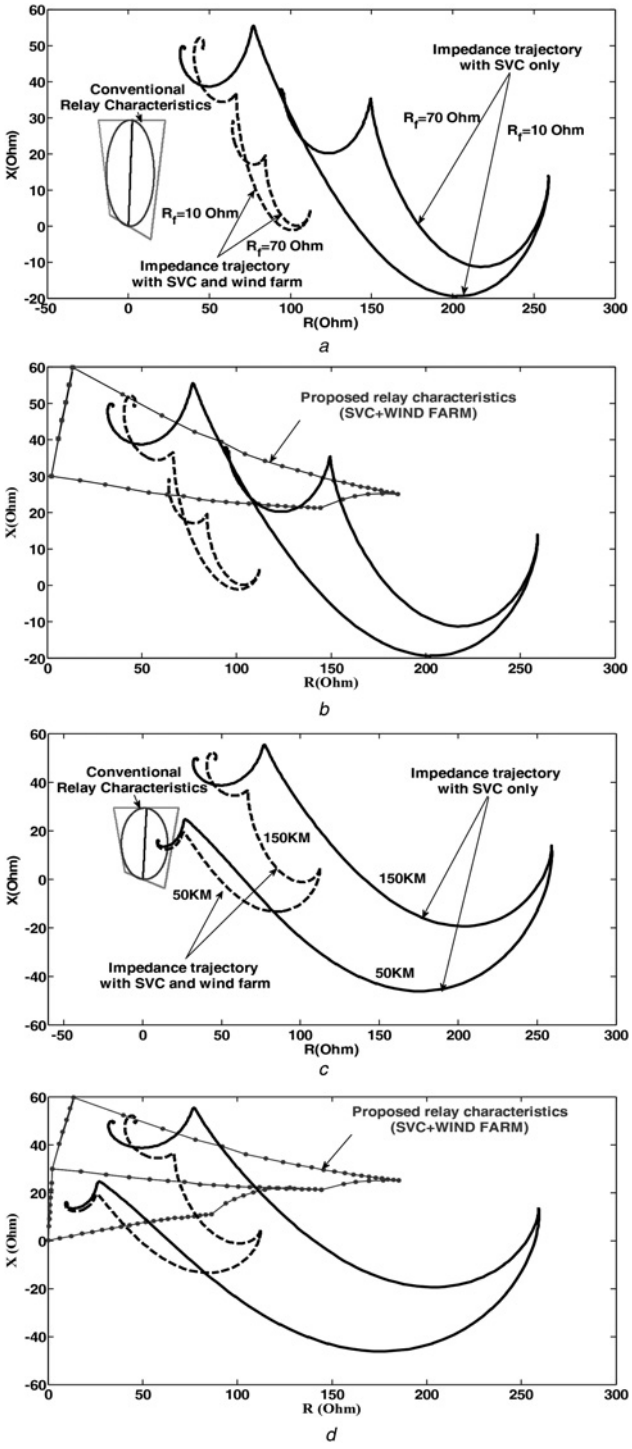

Fig. 7 *Effect of fault resistance in presence of SVC installed in relay end*

a Performance assessments of conventional distance relaying scheme in presence of SVC with different fault resistances
b Performance assessments of the proposed distance relaying scheme in presence of SVC with different fault resistances
c Performance assessments of conventional distance relaying scheme in presence of SVC with different fault locations
d Performance assessments of the proposed distance relaying scheme in presence of SVC with different fault locations

at different positions have been studied, and the A–G element of the system with and without WF together with the conventional mho or quadrilateral characteristic are shown in Fig. 8*c*. It is apparent that when the fault is on the left side of STATCOM (i.e. before STATCOM), the apparent impedance seen by the distance relay is almost the same as that of the system without STATCOM. However, when the fault is on the right side of STATCOM (i.e.

Table 3 Comparative assessment for power system model including SVC with effect of fault resistance

Cases	Relay characteristics	Fault resistance ($R_f = 10\ \Omega$)	Fault resistance ($R_f = 70\ \Omega$)
SVC	conventional mho [8–15]	no trip	no trip
	conventional quadrilateral	no trip	no trip
	proposed	trip	trip
SVC + WF	conventional mho [8–15]	no trip	no trip
	conventional quadrilateral	no trip	no trip
	proposed	trip	trip

after STATCOM), both the apparent resistance and reactance of the system with STATCOM are larger than that of the system without STATCOM. This happens because due to the reactive power injection by STATCOM, the voltage at the STATCOM connecting point is higher compared with the system without STATCOM. That means as seen by the distance relay, the fault is further away than the real distance and an increase in the apparent impedance will lead to the under reaching of distance relay. The relay characteristics of the proposed distance relay is shown in Fig. 8*d* which works effectively. Table 6 presents the performance measurements of the proposed scheme in presence of STATCOM with effect of fault location.

The proposed study decides the tripping boundary of the relay adaptively with respect to changes in power system conditions. In this paper, the basic mathematical formulation is outlined for generating trip boundary including FACTS and off-shore WFs. The trip boundary considered here is of quadrilateral characteristic on an impedance plane obtained by varying fault location and fault resistance within their limits. The proposed scheme has been extensively tested and compared with conventional relays as depicted in Table 3 through Table 6 and found to be highly effective in situations where the conventional relays fail. This shows the potential ability of the proposed adaptive scheme for effective transmission system relaying including FACTS and off-shore wind integration.

7 Conclusions

The proposed research focused on generating the adaptive distance protection scheme for most likely occurring A–G fault in presence of off-shore wind-farm integration with grid employing shunt-FACTS devices such as SVC and STATCOM. The difficulties appear as wind speed varies with time, affecting the power and voltage at relying point. Similarly, it is observed that in presence of shunt-FACTS devices, the trip region is affected by coupling transformer connection. There is a significant variation in apparent impedance between STATCOM and SVC as there is no contribution of zero sequence current by STATCOM during fault as STATCOM system zero sequence impedance is infinite (open circuit) compared with that of SVC. Furthermore, chances of under reaching are more for SVC than that of STATCOM even for same rating of compensation. The proposed approach uses local relaying end information for generating the tripping zone and found highly effective considering wide variations in operating parameters of the WF.

Table 4 Comparative assessment for power system model including SVC with effect of fault location

Cases	Relay characteristics	Fault locations (25% of line)	Fault locations (75% of line)
SVC	conventional mho [8–15]	trip	no trip
	conventional quadrilateral	trip	no trip
	proposed	trip	trip
SVC + WF	conventional mho [8–15]	trip	no trip
	conventional quadrilateral	trip	no trip
	proposed	trip	trip

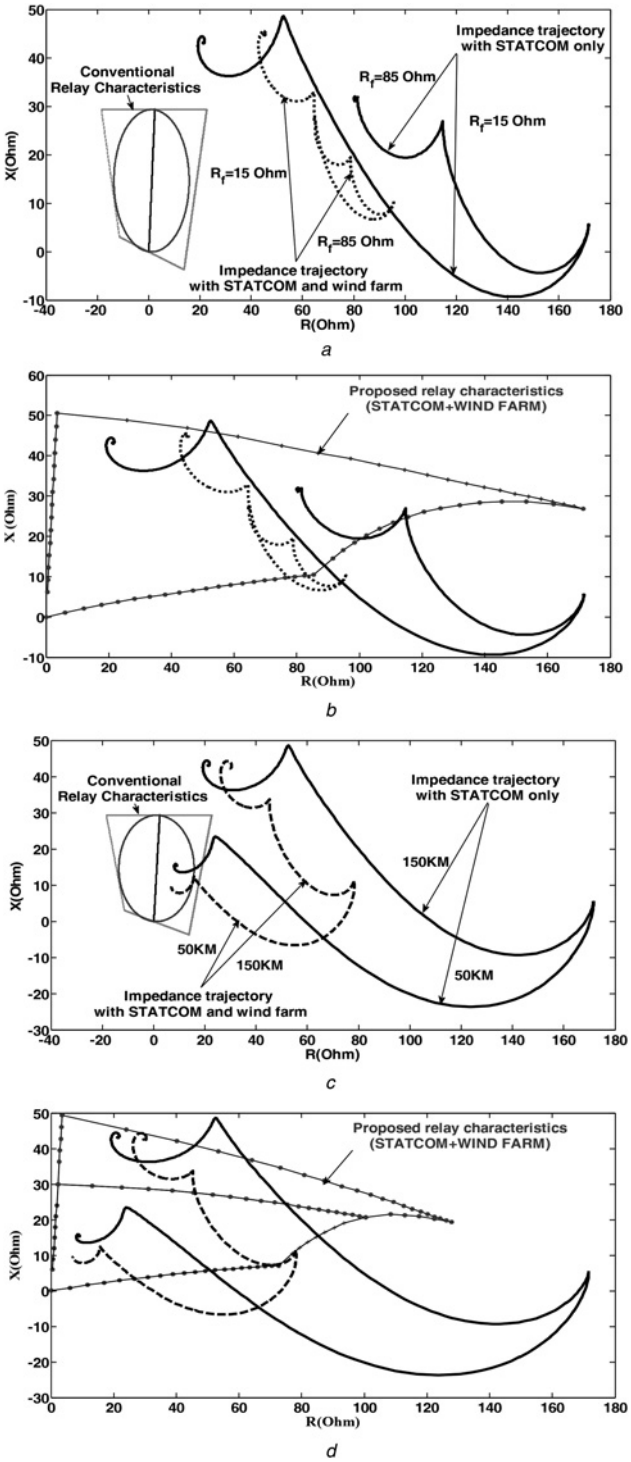

Fig. 8 *Effect of fault resistance in presence of STATCOM installed in relay end*

a Performance assessments of conventional distance relaying scheme in presence of STATCOM with different fault resistances
b Performance assessments of the proposed distance relaying scheme in presence of STATCOM with different fault locations
c Performance assessments of conventional distance relaying scheme in presence of STATCOM with different fault locations
d Performance assessments of the proposed distance relaying scheme in presence of STATCOM with different fault locations

Table 5 Comparative assessment for power system model including STATCOM with effect of fault resistance

Cases	Relay characteristics		Fault resistance (R_f = 15 Ω)	Fault resistance (R_f = 85 Ω)
STATCOM	conventional mho	[8–15]	no trip	no trip
	conventional quadrilateral		no trip	no trip
	proposed		trip	trip
STATCOM + WF	conventional mho	[8–15]	no trip	no trip
	conventional quadrilateral		no trip	no trip
	proposed		trip	trip

Table 6 Comparative assessment for power system model including STATCOM with effect of fault location

Cases	Relay characteristics		Fault locations (25% of line)	Fault locations (75% of line)
STATCOM	conventional mho	[8–15]	trip	no trip
	conventional quadrilateral		trip	no trip
	proposed		trip	trip
STATCOM + WF	conventional mho	[8–15]	trip	no trip
	conventional quadrilateral		trip	no trip
	proposed		trip	trip

8 Acknowledgments

This research work is supported by the Prime Minister's Fellowship for Doctoral Research and being implemented jointly by Science & Engineering Research Board (SERB) and Confederation of Indian Industry (CII), with industry partner Robert Bosch.

9 References

1 Jang, S.I., Choi, J.H., Kim, J.W., *et al.*: 'An adaptive relaying for the protection of a wind farm interconnected with distribution networks'. Proc. IEEE PES Transmission Distribution Conf. Exposition, 7–12 September 2003, vol. 1, pp. 296–302
2 Ma, J., Wang, X., Zhang, Y., *et al.*: 'A novel adaptive current protection scheme for distribution systems with distributed generation', *Int. J. Electr. Power Energy Syst.*, 2012, **43**, pp. 1460–1466
3 Brahma, S.M., Girgis, A.A.: 'Development of adaptive protection schemes for distribution systems with high penetration of distribution generation', *IEEE Trans. Power Deliv.*, 2004, **19**, (1), pp. 56–63
4 Pradhan, A.K., Jóos, G.: 'Adaptive distance relay setting for lines connecting wind farms', *IEEE Trans. Energy Convers.*, 2007, **22**, (1), pp. 206–213
5 Sadeghi, H.: 'A novel method for adaptive distance protection of transmission line connected to wind farms', *Int. J. Electr. Power Energy Syst.*, 2012, **43**, pp. 1376–1382
6 Dubey, R.K., Samantaray, S.R., Panigrahi, B.K.: 'Adaptive distance relaying scheme for transmission network connecting wind farms', *Electr. Power Compon. Syst.*, 2014, **42**, (11), pp. 1181–1193
7 Hingorani, N.G., Gyugyi, L.: 'Understanding FACTS: concepts and technology of flexible AC transmission systems' (Wiley, New York, 1999)
8 Zhou, X.Y., Wang, H.F., Aggarwal, R.K., *et al.*: 'The impact of STATCOM on distance relay'. 15th PSCC, Liege, 22–26 August 2005
9 Sidhu, T.S., Varma, R.K., Gangadharan, P.K., *et al.*: 'Performance of distance relays on shunt – facts compensated transmission lines', *IEEE Trans. Power Deliv.*, 2005, **20**, (3), pp. 1837–1845
10 Albasri, F.A., Sidhu, T.S., Varma, R.K.: 'Impact of shunt-FACTS on distance protection of transmission lines'. Proc. Power Systems Conf., Clemson, SC, 14–17 March 2006
11 Albasri, F.A., Sidhu, T.S., Varma, R.K.: 'Performance comparison of distance protection schemes for shunt-FACTS compensated transmission lines', *IEEE Trans. Power Deliv.*, 2007, **22**, (4), pp. 2116–2125
12 El-Arroudi, K., Joos, G., McGillis, D.T.: 'Operation of impedance protection relays with the STATCOM', *IEEE Trans. Power Deliv.*, 2002, **17**, (2), pp. 381–387
13 Ghorbani, A., Khederzadeh, M., Mozafari, B.: 'Impact of SVC on the protection of transmission lines', *Int. J. Electr. Power Energy Syst.*, 2012, **42**, pp. 702–709
14 Singh, A.R., Dambhare, S.S.: 'Adaptive distance protection of transmission line in presence of SVC', *Int. J. Electr. Power Energy Syst.*, 2013, **53**, pp. 78–84
15 Singh, A.R., Patne, N.R., Kale, V.S.: 'Adaptive distance protection setting in presence of mid-point STATCOM using synchronized measurement', *Int. J. Electr. Power Energy Syst.*, 2015, **67**, pp. 252–260
16 Biswal, M., Pati, B.B., Pradhan, A.K.: 'Adaptive distance relay setting for series compensated line', *Int. J. Electr. Power Energy Syst.*, 2013, **52**, pp. 198–206
17 Dubey, R., Samantaray, S.R., Panigrahi, B.K.: 'Simultaneous impact of unified power flow controller and off-shore wind penetration on distance relay characteristics', *IET Gener. Transm. Distrib.*, 2014, **8**, (11), pp. 1869–1880
18 Dubey, R., Samantaray, S.R., Panigrahi, B.K., *et al.*: 'Adaptive distance relay setting for parallel transmission network connecting wind farms and UPFC', *Int. J. Electr. Power Energy Syst.*, 2015, **65**, pp. 113–123
19 Sarangi, S., Pradhan, A.K.: 'Adaptive direct under reaching transfer trip protection scheme for three-terminal line', *IEEE Trans. Power Deliv.*, 2015, **PP**, (99), DOI: 10.1109/TPWRD.2015.2388798
20 Ma, J., Ma, W., Qiu, Y., *et al.*: 'An adaptive distance protection scheme based on the voltage drop equation', *IEEE Trans. Power Deliv.*, 2015, **30**, (4), pp. 1931–1940
21 Available http://www.opal-rt.com
22 MATLAB Sim Power Systems User's Guide, Version 4.6 (R2008a). Available at http://www.mathworks.com/access/helpdesk/help/toolbox/physmod/powersys, accessed 1 December 2012
23 Ekanayake, J.B., Holds worth, L., Wu, X., *et al.*: 'Dynamic modeling of doubly fed induction generator wind turbines', *IEEE Trans. Power Syst.*, 2003, **18**, (2), pp. 803–809
24 Jena, M.K., Samantaray, S.R.: 'Data-mining-based intelligent differential relaying for transmission lines including UPFC and wind farms', *IEEE Trans. Neural Netw. Learn. Syst.*, 2015, early access

10 Appendices

10.1 Appendix 1

$$I_f = \frac{V_{\text{prefault\_f}}}{Z_1 + Z_2 + Z_0 + 3R_f} \tag{1}$$

$$I_1 = I_2 = I_0 = I_f \tag{2}$$

$$Z_1 = \frac{(Z_{1s} + xZ_{1L}) \times (Z_{1r} + (1-x)Z_{1L})}{(Z_{1s} + xZ_{1L}) + (Z_{1r} + (1-x)Z_{1L})} \tag{3}$$

$$Z_2 = Z_1 \tag{4}$$

$$Z_0 = \frac{(Z_{0s} + xZ_{0L}) \times (Z_{0r} + (1-x)Z_{0L})}{(Z_{0s} + xZ_{0L}) + (Z_{0r} + (1-x)Z_{0L})} \tag{5}$$

$$I_{r1} = I_1 \times \frac{(1-x)Z_{1L} + Z_{1r}}{(Z_{1s} + xZ_{1L}) + (Z_{1r} + (1-x)Z_{1L})} \tag{6}$$

$$I_{r2} = I_{r1} \tag{7}$$

$$I_{r0} = I_0 \times \frac{(1-x)Z_{0L} + Z_{0r}}{(Z_{0s} + xZ_{0L}) + (Z_{0r} + (1-x)Z_{0L})} \tag{8}$$

$$I_{\text{relay}} = I_{\text{prefault\_R}} + I_{r1} + I_{r2} + I_{r0} \tag{9}$$

$$V_{\text{postfault\_R}} = (I_1 + I_2 + I_0)R_f + (I_{\text{prefault\_R}} + I_{r1} + I_{r2})xZ_{1L} + I_{r0}xZ_{0L} \tag{10}$$

$$Z_{\text{APPARENT}} = \frac{V_{\text{postfault\_R}}}{I_{\text{relay}} + (\{Z_{0L} - Z_{1L}\}/Z_{1L})I_{r0}} \tag{11}$$

Equation (11) represents the apparent impedance calculation for uncompensated transmission line.

10.2 Appendix 2

$$Z_{\text{SVC}} = \frac{V_{\text{ref}}^2}{P_{\text{SVC}}}$$
$$Z_{Xr} = \frac{V_{\text{HV}}^2}{P_{Xr}} \times \%\text{impedance} \tag{12}$$

$$Z_{\text{sh1}} = Z_{\text{SVC}} + Z_{Xr} \tag{13}$$

$$Z_{sh2} = Z_{sh1} \tag{14}$$

$$Z_{xr0} = Z_{xr} \tag{15}$$

$$Z_{S1} = \frac{Z_{1s} \times Z_{sh1}}{Z_{1s} + Z_{sh1}} \tag{16}$$

$$Z_{S2} = Z_{S1} \tag{17}$$

$$Z_1 = \frac{(Z_{S1} + xZ_{1L}) \times (Z_{1r} + (1-x)Z_{1L})}{(Z_{S1} + xZ_{1L}) + (Z_{1r} + (1-x)Z_{1L})} \tag{18}$$

$$Z_2 = Z_1 \tag{19}$$

$$Z_{S0} = \frac{Z_{0s} \times Z_{xr0}}{Z_{0s} + Z_{xr0}} \tag{20}$$

$$I_f = \frac{V_{prefault\_f}}{Z_1 + Z_2 + Z_0 + 3R_f} \tag{21}$$

$$I_1 = I_2 = I_0 = I_f \tag{22}$$

$$I_{S1} = I_1 \times \frac{(1-x)Z_{1L} + Z_{1r}}{(Z_{S1} + xZ_{1L}) + (Z_{1r} + (1-x)Z_{1L})} \tag{23}$$

$$I_{S2} = I_{S1} \tag{24}$$

$$I_{S0} = I_0 \times \frac{(1-x)Z_{0L} + Z_{0r}}{(Z_{S0} + xZ_{0L}) + (Z_{0r} + (1-x)Z_{0L})} \tag{25}$$

$$I_{r1} = I_{S1} \times \frac{Z_{sh1}}{Z_{sh1} + Z_{1s}} \tag{26}$$

$$I_{r2} = I_{r1} \tag{27}$$

$$I_{r0} = I_{S0} \times \frac{Z_{SVC}}{Z_{SVC} + Z_{0s}} \tag{28}$$

$$I_{relay} = I_{prefault\_R} + I_{r1} + I_{r2} + I_{r0} \tag{29}$$

$$V_{postfault\_R} = (I_1 + I_2 + I_0)R_f + (I_{prefault\_R} + I_{S1} + I_{S2})xZ_{1L} + I_{S0}xZ_{0L} \tag{30}$$

$$Z_{APPARENT} = \frac{V_{postfault\_R}}{I_{relay} + (\{Z_{0L} - Z_{1L}\}/Z_{1L})I_{r0}} \tag{31}$$

10.3 Appendix 3

$$Z_{STATCOM} = \frac{V_{ref}^2}{P_{STATCOM}} \tag{32}$$

$$Z_{Xr} = \frac{V_{HV}^2}{P_{Xr}} \times \%\text{impedance} \tag{33}$$

$$Z_{sh1} = Z_{STATCOM} + Z_{Xr} \tag{34}$$

$$Z_{sh2} = Z_{sh1} \tag{35}$$

$$Z_{S1} = \frac{Z_{1s} \times Z_{sh1}}{Z_{1s} + Z_{sh1}} \tag{36}$$

$$Z_{S2} = Z_{S1} \tag{37}$$

$$Z_1 = \frac{(Z_{S1} + xZ_{1L}) \times (Z_{1r} + (1-x)Z_{1L})}{(Z_{S1} + xZ_{1L}) + (Z_{1r} + (1-x)Z_{1L})} \tag{38}$$

$$Z_2 = Z_1 \tag{39}$$

$$Z_0 = \frac{(Z_{0s} + xZ_{0L}) \times (Z_{0r} + (1-x)Z_{0L})}{(Z_{0s} + xZ_{0L}) + (Z_{0r} + (1-x)Z_{0L})} \tag{40}$$

$$I_f = \frac{V_{prefault\_f}}{Z_1 + Z_2 + Z_0 + 3R_f} \tag{41}$$

$$I_1 = I_2 = I_0 = I_f \tag{42}$$

$$I_{S1} = I_1 \times \frac{(1-x)Z_{1L} + Z_{1r}}{(Z_{S1} + xZ_{1L}) + (Z_{1r} + (1-x)Z_{1L})} \tag{43}$$

$$I_{S2} = I_{S1} \tag{44}$$

$$I_{S0} = I_0 \times \frac{(1-x)Z_{0L} + Z_{0r}}{(Z_{0s} + xZ_{0L}) + (Z_{0r} + (1-x)Z_{0L})} \tag{45}$$

$$I_{r0} = I_{S0} \tag{46}$$

$$I_{r1} = I_{S1} \times \frac{Z_{sh1}}{Z_{sh1} + Z_{1s}} \tag{47}$$

$$I_{r2} = I_{r1} \tag{48}$$

$$I_{relay} = I_{prefault\_R} + I_{r1} + I_{r2} + I_{r0} \tag{49}$$

$$V_{postfault\_R} = (I_1 + I_2 + I_0)R_f + (I_{prefault\_R} + I_{S1} + I_{S2})xZ_{1L} + I_{S0}xZ_{0L} \tag{50}$$

$$Z_{APPARENT} = \frac{V_{postfault\_R}}{I_{relay} + (\{Z_{0L} - Z_{1L}\}/Z_{1L})I_{r0}} \tag{51}$$